AD-A080 442 CINCINNATI UNIV OH DEPT OF AEROSPACE ENGINEERING AND--ETC F/G 20/4
ON STRONG SLOT INJECTION INTO A SUBSONIC LAMINAR BOUNDARY LAYER--ETC(U)
NOV 78 M NAPOLITANO, R E MESSICK N00014-76-C-0359
UNCLASSIFIED AFL-78-11-44 NL

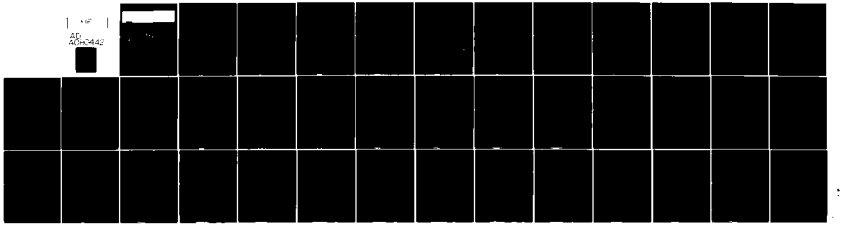

END
DATE FILMED
3-80
DDC

REPORT NO. AFL 78-11-44

ON STRONG SLOT INJECTION INTO A SUBSONIC LAMINAR BOUNDARY LAYER

LEVEL II

M. NAPOLITANO AND R.E. MESSICK

This research was supported by the Naval Sea Systems Command General Hydromechanics Research Program administered by the David W. Taylor Naval Ship Research and Development Center under Contract N00014-76-C-0359.

November 1978

SECURITY CLASSIFICATION OF THIS PAGE *(When Data Entered)*

REPORT DOCUMENTATION PAGE	READ INSTRUCTIONS BEFORE COMPLETING FORM
1. REPORT NUMBER: AFL-78-11-44	2. GOVT ACCESSION NO.	3. RECIPIENT'S CATALOG NUMBER
4. TITLE *(and Subtitle)*: ON STRONG SLOT INJECTION INTO A SUBSONIC LAMINAR BOUNDARY LAYER	5. TYPE OF REPORT & PERIOD COVERED: 1978
	6. PERFORMING ORG. REPORT NUMBER
7. AUTHOR(s): M. Napolitano & R. E. Messick	8. CONTRACT OR GRANT NUMBER(s): N00014-76-C-0359
9. PERFORMING ORGANIZATION NAME AND ADDRESS: Department of Aerospace Engineering and Applied Mechanics, University of Cincinnati	10. PROGRAM ELEMENT, PROJECT, TASK AREA & WORK UNIT NUMBERS: 61153N RO2301 SR 023 01 01
11. CONTROLLING OFFICE NAME AND ADDRESS: David W. Taylor Naval Ship R&D Center(Code 1505) Bethesda, Md 20084	12. REPORT DATE: November 1978
	13. NUMBER OF PAGES: 33
14. MONITORING AGENCY NAME & ADDRESS *(if different from Controlling Office)*: Office of Naval Research 800 N. Quincy St Arlington, Va 22217	15. SECURITY CLASS. *(of this report)*: UNCLASSIFIED
	15a. DECLASSIFICATION/DOWNGRADING SCHEDULE

16. DISTRIBUTION STATEMENT *(of this Report)*

APPROVED FOR PUBLIC RELEASE: DISTRIBUTION UNLIMITED

17. DISTRIBUTION STATEMENT *(of the abstract entered in Block 20, if different from Report)*

18. SUPPLEMENTARY NOTES

Sponsored by the Naval Sea Systems Command General Hydromechanics Research (GHR) Program administered by the David W. Taylor Naval Ship R&D Center, Code 1505, Bethesda, Md 20084

19. KEY WORDS *(Continue on reverse side if necessary and identify by block number)*

Laminar Boundary Layer
Asymptotically High Reynolds Number
GHR Program
Fourier Transform techniques

20. ABSTRACT *(Continue on reverse side if necessary and identify by block number)*

This document is concerned with the problem of strong slot injection into a subsonic laminar boundary layer at asymptotically high Reynolds number. The problem is formulated and the governing equations are presented within the context of triple deck theory. The linear problem, valid when the injection velocity is small, is solved analytically by Fourier Transform techniques. Graphical results are given for a wide range of slot lengths. A numerical technique for the nonlinear equations is presented and used to

DD FORM 1 JAN 73 1473 EDITION OF 1 NOV 65 IS OBSOLETE
S/N 0102-LF-014-6601

SECURITY CLASSIFICATION OF THIS PAGE *(When Data Entered)*

obtain solutions for various injection velocities. Sepration is found to first occur downstream of the slot, where a recirculating flow bubble is formed.

ON STRONG SLOT INJECTION INTO A SUBSONIC LAMINAR BOUNDARY LAYER

M. Napolitano* and R.E. Messick**

Aerospace Engineering and Applied Mechanics Department
University of Cincinnati
Cincinnati, Ohio 45221

This research was supported by the Naval Sea Systems Command General Hydromechanics Research Program administered by the David W. Taylor Naval Ship Research and Development Center under Contract N00014-76-C-0359.

---

* Research Associate; also Assistant Professor at the University of Bari, Italy.

** Associate Professor, Department of Engineering Science, University of Cincinnati, Cincinnati, Ohio.

ON STRONG SLOT INJECTION INTO A SUBSONIC LAMINAR BOUNDARY LAYER

M. Napolitano and R.E. Messick

ABSTRACT

This paper is concerned with the problem of strong slot injection into a subsonic laminar boundary layer at asymptotically high Reynolds number. The problem is formulated and the governing equations are presented within the context of triple deck theory. The linear problem, valid when the injection velocity is small, is solved analytically by Fourier Transform techniques. Graphical results are given for a wide range of slot lengths. A numerical technique for the nonlinear equations is presented and used to obtain solutions for various injection velocities. Separation is found to first occur downstream of the slot, where a recirculating flow bubble is formed.

TABLE OF CONTENTS

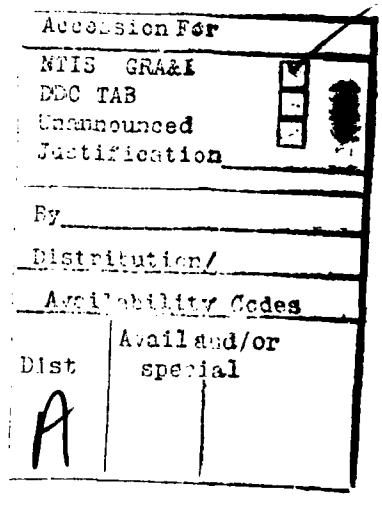

LIST OF FIGURES

I. INTRODUCTION

Injection of a secondary fluid into a well developed boundary layer is a widely used technique in the aeronautical industry. It is used, for example, for cooling gas turbine blades and for controlling transition and/or separation (blow off) of the boundary layer over airplane control surfaces. It is therefore of great practical significance, for the aerodynamicist and the thermal analyst as well, to be able to analytically predict the effect of injection on the flow pattern and temperature distribution around a turbine blade or any other piece of machinery. Our interest is presently limited to the aerodynamic aspect of the problem. In this respect, most of the early, classical work on injection is concerned with the case of weak blowing into an incompressible, laminar boundary layer; that is, the ratio between injection and free stream velocities is assumed to be inversely proportional to the square root of the characteristic Reynolds number, Re. For this case, classical boundary layer theory is valid and self similar solutions are possible [1]. The most important conclusion of such studies is that weak injection has a much greater effect on the boundary layer properties (wall shear, displacement thickness etc) than one might expect, and such injection can even blow the layer off the plate, i.e. induce separation. Subsequently, the interest of most researchers has been attracted by the supersonic mainstream case. See Smith and Stewartson [4] for a critical review of their efforts. In particular, after the formalization of the asymptotic triple deck theory of Stewartson et al. [2,3] a rigorous definition for moderate and strong blowing has become available, together with the appropriate governing equations. Smith and Stewartson [4] consider the problem of strong slot injection into a supersonic laminar boundary layer; for this, they provide analytical

solutions to the linear problem, valid when the injection velocity is small in the triple deck scaling, and a numerical technique for the full nonlinear problem. Such a numerical technique, though, developed a "pressure sensitivity" or instability, due to ineffective imposition of the downstream boundary condition, and could not account for separation ahead of the slot. Napolitano [6] has recently overcome these two difficulties and provided more complete results, in which separation is indeed found to first occur ahead of the slot. Finally, Smith and Stewartson [5] also considered the problem of strong (and massive) plate injection into a separated supersonic laminar boundary layer.

Sychev [7] has recently shown that triple deck theory is valid for subsonic flow conditions as well. The problem of strong slot injection into a subsonic laminar boundary layer, has thus become feasible, and is the subject of this paper. In section II the problem is defined and the triple deck governing equations presented. In section III, the case in which the injection velocity is small, is considered: the governing equations are linearised and solved analytically by Fourier transform Techniques. In section IV a numerical technique for the full nonlinear problem, derived from that of Napolitano et al [8], is presented. Finally, in section V results are provided for the linear and nonlinear problems. Linear pressure and wall shear solutions are presented for a wide range of slot lengths. Nonlinear results are instead provided for one slot length only but for various values of the injection velocity.

II. Problem Definition and Governing Equations

A Newtonian fluid, of kinematic viscosity ν^*, flows past a semiinfinite flat plate with subsonic free stream velocity, U_∞^*, parallel to the plate. At a distance x_o^* from the leading edge of the plate, fluid is injected perpendicular to the wall, with velocity v_w^*, thru a slot of length $x_s^* - x_o^*$. The characteristic Reynolds number, $Re = U_\infty^* x_o^*/\nu^*$, is asymptotically large and the injection velocity and slot lengths are of order $Re^{-3/8} U_\infty^*$ and $Re^{-3/8} x_o^*$, respectively. For this flow situation, (see Figure 1) three region or decks develop around the injection region, the lower, middle and outer decks, all having the characteristic length of the interaction region, of order $\varepsilon^3 x_o^*$ ($\varepsilon = Re^{-1/8}$) and characteristic height of order $\varepsilon^5 x_o^*$, $\varepsilon^4 x_o^*$ and $\varepsilon^3 x_o^*$ respectively. The middle deck is a displaced Blasius boundary layer, having the passive role of communicating the pressure interaction between inner and outer decks. This last one is a potential flow past a "thin airfoil" produced by the viscous effects in the lower deck underneath. The inner (lower) deck, finally, is a viscous region which arises from the need to satisfy the wall boundary conditions on the plate. After appropriate scaling of the independent and dependent variables and proper matching between the neighboring decks, the Navier Stokes equations reduce to the triple deck ones. These are basically the lower deck boundary layer like equations coupled to the outer deck (linear airfoil) pressure interaction law. The continuity and momentum equations are given as:

$$u_x + v_y = 0; \quad u\,u_x + v\,u_y = -\frac{dp}{dx} + u_{yy}; \qquad (2.1,a,b)$$

with boundary conditions:

$$u(x,0) = 0 \tag{2.2}$$

$$v(x,0) = \begin{cases} V_w & \text{for } 0 < x \leq x_s \\ 0 & \text{elsewhere} \end{cases} \tag{2.3}$$

$$u(x,y \to \infty) \to y + \delta, \tag{2.4}$$

$$u(x \to -\infty, y) \to y . \tag{2.5}$$

The pressure displacement interaction law is finally given by

$$\delta_{xx} = \frac{-1}{\pi} \oint_{-\infty}^{\infty} \frac{p_\xi d\xi}{x-\xi} , \tag{2.6}$$

where the integral denotes the Cauchy principal value. Note that δ is the total displacement, due to the viscous effects and to the injected fluid as well. Also note that δ and p are independent of the normal coordinate y. For these two quantities the x subscript indicates a total (rather than a partial) derivative.

III. Solution to the Linear Problem

The problem described by equations (2.1) thru (2.6) is nonlinear, because of the convective terms $u\,u_x$ and $v\,u_y$ in the momentum equation (2.1b) and, at present, can be solved only numerically. The case in which the injection velocity V_w is very small ($V_w \ll 1$), however, can be studied analytically. This analytical solution is very important since it provides interesting information on the asymptotic decay of the solution for $x \to \pm \infty$ and is the only tool for assessing accuracy and reliability of the numerical results. Moreover, its usefulness can be reasonably expected to be even greater, because, for the supersonic mainstream case, it has been found that the linear solution is relatively close to the full nonlinear one, for V_w as large as 1 [6] . A broad range of validity for the linear solution has also been found for both supersonic and subsonic flow past a hump on a flat plate [8,9]. For V_w equal to zero, the flow field is one characterised by uniform shear (u=y) with v, p and δ identically equal to zero. For $V_w \ll 1$, thus, the solution is a small perturbation of such a uniform shear flow, that is

$$u(x,y) = y + V_w\,\bar{u}\,(x,y) + \ldots \tag{3.1}$$

$$v(x,y) = V_w\bar{v}(x,y) + \ldots \tag{3.2}$$

$$\delta(x,y) = V_w\bar{\delta}(x,y) + \ldots \tag{3.3}$$

$$p(x,y) = V_w\bar{p}(x,y) + \ldots \tag{3.4}$$

In order to obtain the governing equations for the linear problem, equations (3.1 - 3.4) are substituted into equations (2.1 - 2.6) and only the terms containing V_w linearly are retained, to give:

$$\bar{u}_x + \bar{v}_y = 0; \; y\,\bar{u}_x + \bar{v} = -\frac{d\bar{p}}{dx} + \bar{u}_{yy} \qquad (3.5\ a,b)$$

$$\bar{u}(x,0) = 0 \qquad (3.6)$$

$$\bar{v}(x,0) = \begin{cases} 1; & 0 \leq x < x_s \\ 0; & \text{elsewhere} \end{cases} \qquad (3.7)$$

$$\bar{u}\,(x, y \to \infty) = \bar{\delta} \qquad (3.8)$$

$$\bar{u}\,(x \to -\infty, y) = 0 \qquad (3.9)$$

$$\frac{d^2\bar{\delta}}{dx^2} = -\frac{1}{\pi} \oint_{-\infty}^{\infty} \frac{\bar{p}_\xi d\xi}{x-\xi} \qquad (3.10)$$

Linearization makes it possible to construct the solution for the case of a finite slot from the solution for the infinite slot ($x_s = \infty$) by translation and superposition. For clarity and convenience the superior bars will be omitted from the dependent variables for the case of the infinite slot.

The infinite slot problem may thus be formulated as follows:

$$u_x + v_y = 0\ , \; y\,u_x + v = -p_x + u_{yy} \qquad (3.11\ a,b)$$

for $(x,y) \in \{(-\infty,\infty)X[0,\infty)\}$, with the subsidiary conditions:

$$u(x.0) = 0 \tag{3.12}$$

$$v(x,0) = h(x) \tag{3.13}$$

$$u(-\infty,y) = 0 \tag{3.14}$$

$$u(x,\infty) = \delta(x) \tag{3.15}$$

$$p(\pm\infty) = 0 \tag{3.16}$$

$$\delta_{xx}(x) = -\frac{1}{\pi} \int_{-\infty}^{\infty} \frac{p_{\xi}(\xi)d\xi}{x-\xi} \tag{3.17}$$

where h(x) denotes the Heaviside step-function and the integral the Cauchy principal value.

The system (3.11) may be transformed to a single equation by differentiating (3.11 b) with respect to y and using (3.11 a) to eliminate v_y. The result is

$$w_{yy} - y\, w_x = 0 \tag{3.18}$$

where $w = u_y$. Let capital letters denote the Fourier transforms of the corresponding (lower-case) dependent variables e.g.

$$W = \int_{-\infty}^{\infty} w\, e^{-i\omega x}\, dx \tag{3.19}$$

The Fourier transform of (3.18) using (3.14) then provides the Airy differential equation

$$W_{yy} - i\omega y\, W = 0 \tag{3.20}$$

where, again for clarity and convenience, the product $i\omega$ will be understood to stand for $\varepsilon + i\omega$, with $\varepsilon > 0$ an arbitrarily small constant to assure convergence of the transform at the upper limit. The limit as $\varepsilon \downarrow 0$ is to be used in all results. The only non-integral powers of $i\omega$ to be encountered here involve the cube root. A natural branch for these, leaving the real ω axis free is

$$\operatorname*{Lin}_{\varepsilon\downarrow 0} [\varepsilon + i\omega]^{\frac{1}{3}} = [i\omega]^{\frac{1}{3}} = |\omega|^{\frac{1}{3}} e^{\frac{1}{3}(\phi+\frac{\pi}{2})} \tag{3.21}$$

for $-\frac{3\pi}{2} < \phi < \frac{\pi}{2}$ which defines the cut indicated in the figure.

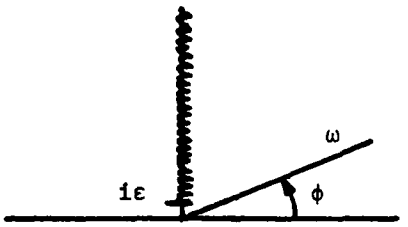

The general solution of (3.20) is usually written as

$$W = C_0\, \mathrm{Ai}\,([i\omega]^{\frac{1}{3}} y) + C_1\, \mathrm{Bi}\,([i\omega]^{\frac{1}{3}} y) \tag{3.22}$$

where C_0, C_1 are constants and Ai, Bi are the Airy functions of the first and second kind, respectively. However, it now follows that W is exponentially

unbounded as $y \to \infty$, violating conditions (3.14) and (3.15), unless $C_1 = 0$. With $C_1 = 0$, condition (3.12) implies that

$$U = C_0 \int_0^y \text{Ai}\left([i\omega]^{\frac{1}{3}}\xi\right)d\xi \tag{3.23}$$

The Fourier transform of (3.15) then requires that

$$\Delta = C_0 \int_0^\infty \text{Ai}\left([i\omega]^{\frac{1}{3}}\xi\right)d\xi \tag{3.24}$$

However, for precisely the branch defined in (3.21), the integral in (3.24) evaluates to $\frac{1}{3[i\omega]^{\frac{1}{3}}}$. Thus,

$$C_0 = 3[i\omega]^{\frac{1}{3}}\,\Delta \tag{3.25}$$

Now Δ is related to P by means of the transform of (3.17), using (3.16). i.e.

$$i\omega\Delta = i\,P\,\text{sgn}\,\omega \tag{3.26}$$

where $\text{sgn}\,\omega = \begin{cases} 1\,, & \omega > 0 \\ -1\,, & \omega < 0 \end{cases}$

Condition (3.13) remains to be satisfied. However, by continuity it can be used with (3.11 b) to give:

$$u_{yy} = p_x + h(x) \quad \text{for} \quad y \to 0 \tag{3.27}$$

The transform of this (with our limiting convention) is

$$U_{yy} = i\omega P + \frac{1}{i\omega} \quad \text{for} \quad y \to 0 \tag{3.28}$$

Substituting from (3.28) for U, we have

$$C_0[i\omega]^{\frac{1}{3}} \, Ai'(0) = i\omega P + \frac{1}{i\omega} \tag{3.29}$$

Equations (3.25), (3.26) and (3.29) maybe solved to give

$$P = \frac{-(i\omega)^{-\frac{2}{3}}}{D} \tag{3.30a}$$

$$C_0 = \frac{-3i(i\omega)^{-\frac{4}{3}} \operatorname{sgn} \omega}{D} \tag{3.30b}$$

$$\Delta = \frac{-i(i\omega)^{-\frac{5}{3}} \operatorname{sgn} \omega}{D} \tag{3.30c}$$

where $D = (i\omega)^{\frac{4}{3}} + \theta^{\frac{4}{3}} i \operatorname{sgn} \omega$ and $\theta = [-3Ai'(0)]^{\frac{3}{4}} = 0.8272 \ldots$ is Lighthill's constant.

U is now known from (3.30b) and (3.23), so its inverse transform u, together with p from (3.30a), maybe used with (3.11) to find v and check the results.

The inverse transforms can be put into a suitable real form after some cumbersome but straight-forward manipulations. These manipulations involve altering the paths of integration to radial lines at angles of $\phi = \pm \frac{\pi}{6}$ in the

ω-plane, depending upon whether or not $\pm x > 0$.

The result for the pressure then takes the compact form:

$$p(x) = \frac{3}{2^{h(x)}\pi\theta} \int_0^\infty \frac{e^{-\theta|x|\rho^3} d\rho}{\rho^8 - \sqrt{3}\,\rho^4 h(x) + 1} \tag{3.31}$$

It now follows by superposition that the pressure for the finite slot is:

$$\bar{p}(x) = p(x) - p(x - x_s) \tag{3.32}$$

It is obvious that $\bar{p}(x)$ is continuous everywhere except possibly at the slot ends i.e. at $x=0, x_s$. Let the jump in a function $f(x)$ be defined as

$$\{f(x)\} = f(x+) - f(x-) \tag{3.33}$$

then

$$\{\bar{p}(0)\} = -\{\bar{p}(x_s)\} = \{p(0)\}$$

$$= \frac{3}{2\pi\theta}\left[\int_0^\infty \frac{d\rho}{\rho^8 - \sqrt{3}\,\rho^4 + 1} - 2\int_0^\infty \frac{d\rho}{\rho^8 + 1}\right]$$

$$= \frac{3}{2\pi\theta}\left[\frac{\sqrt{2}\pi\cos\frac{\pi}{8}}{2} - 2\,\frac{\sqrt{2}\pi\cos\frac{\pi}{8}}{4}\right] = 0 \tag{3.34}$$

Also,

$$\{\bar{p}_x(0)\} = -\{\bar{p}_x(x_s)\} = \{p_x(0)\}$$

$$= -\frac{3}{2\pi}\left[\int_0^\infty \frac{\rho^3 d\rho}{\rho^8-\sqrt{3}\rho^4+1} + 2\int_0^\infty \frac{\rho^3 d\rho}{\rho^8+1}\right]$$

$$= -\frac{3}{2\pi}\left[\frac{5\pi}{12} + 2\,\frac{\pi}{8}\right] = -1 \qquad (3.35)$$

This shows that $\bar{p}$ is (i.e. may be defined to be!) continuous on $(-\infty,\infty)$, but that its derivative, the pressure gradient, displays unit jump discoutinuities at the ends of the slot in opposite directions.

Considering (3.31) and (3.32), it is seen that outside of the slot the denominators of both integrands in (3.32) are the same. (Note that $\rho^8 - \sqrt{3}\rho^4 + 1 > 0$ for all ρ so $p(x) > 0$ for all x.) However, for $x < 0$ the exponential function in the integrand of $p(x)$ exceeds that in $p(x-x_s)$. The situation is reversed for $x > x_s$.

It follows then, because of the difference in p's in (3.32), that $\bar{p}(x)$ is positive to the left of the slot ($x<0$) and negative to the right of the slot ($x>x_s$). Also, differentiation of $\bar{p}(x)$ for $x < 0$ does not alter this sign relationship while for $x > x_s$ it reverses it. This means that in both cases $\bar{p}(x)$ is a monotone increasing function of x. Now $\bar{p}(\pm\infty) = 0$, so that $p(x)$ starts from zero at $x = -\infty$ and increases positively to the <u>maximum</u> of $\bar{p}(0) > 0$ at $x = 0$. To the right of the slot $\bar{p}(x)$ starts at the negative value $\bar{p}(x_s)$ for $x = x_s$ and increases to zero as $x \to \infty$.

Within the slot, differentiation of $\bar{p}(x)$ results in the derivative of $p(x)$ being negative while the derivative of $p(x-x_s)$ remains positive. This means that the derivative of $\bar{p}(x)$ within the slot is negative and that $\bar{p}(x)$ is monotone decreasing from $\bar{p}(0) > 0$ to the minimum of $\bar{p}(x_s) < 0$ at the r.h. end of the slot.

Finally, it is clear that for $x \leq 0$, $\bar{p}(x)$ is a monotone increasing function or x_s. The maximum $\bar{p}(0)$ increases from 0 for $x_s = 0$ to the maximum $p(0) = \frac{3\sqrt{2}}{4\theta} \cos\frac{\pi}{8}$, (see (3.34)), for $x_s \uparrow \infty$. Conversely, for $x \geq x_s$, $\bar{p}(x)$ is a monotone decreasing function of x_s. The minimum $\bar{p}(x_s)$ decreases from 0 for $x_s = 0$ to the minimum $-p(0) = -\frac{3\sqrt{2}}{4\theta} \cos\frac{\pi}{8}$ for $x_s \uparrow \infty$.

The skin friction coefficient $\bar{\tau}(x) = \bar{u}_y(x,0)$ is also of primary importance. For the infinite slot $\tau(x) = u_y(x,0)$ can be written in the compact form:

$$\tau(x) = -\frac{9\sqrt{3}}{2\pi^2\theta^3}\left[\frac{\pi(\theta x)^{\frac{1}{3}}}{\Gamma(\frac{1}{3})}h(x) + \int_0^\infty \frac{\rho^2 e^{-\theta|x|\rho^3\sqrt{3}(2\rho^4-1)}h(x)}{\rho^8 - \sqrt{3}\rho^4 h(x) + 1}\,d\rho\right] \quad (3.36)$$

So that, as before, for the <u>finite</u> slot;

$$\bar{\tau}(x) = \tau(x) - \tau(x-x_s) \quad (3.37)$$

Here too $\bar{\tau}(x)$ is obviously continuous except possibly at the slot ends.

$$\{\bar{\tau}(0)\} = -\{\bar{\tau}(x_s)\} = \{\tau(0)\}$$

$$= -\frac{9\sqrt{3}}{2\pi^2\theta^3}\left[\int_0^\infty \frac{\rho^2(\sqrt{\frac{3}{2}}\,\rho^4 - 1)d\rho}{\rho^8 - \sqrt{3}\rho^4 + 1} - \int_0^\infty \frac{\rho^2 d\rho}{\rho^8+1}\right]$$

$$= -\frac{9\sqrt{3}}{2\pi^2\theta^3}\left[\frac{\pi\sqrt{2}\,\sin\frac{\pi}{8}}{4} - \frac{\pi\sqrt{2}\,\sin\frac{\pi}{8}}{4}\right] = 0 \qquad (3.38)$$

Also,

$$\tau_x(x) = -\frac{9\sqrt{3}}{2\pi^2\theta^2}\left(-\frac{1}{2}\right)^{h(x)}\int_0^\infty \frac{[\rho^5 - \sqrt{3}\rho h(x)]e^{-\theta|x|\rho^3}\,d\rho}{\rho^8 - \sqrt{3}\rho^4 h(x) + 1} \qquad (3.39)$$

Therefore:

$$\{\bar{\tau}_x(0)\} = -\{\bar{\tau}_x(x_s)\} = \{\tau_x(0)\}$$

$$= -\frac{9\sqrt{3}}{2\pi^2\theta^2}\left[-\frac{1}{2}\int_0^\infty \frac{(\rho^5 - \sqrt{3}\rho)d\rho}{\rho^8 - \sqrt{3}\rho^4 + 1} - \int_0^\infty \frac{\rho^5 d\rho}{\rho^8+1}\right]$$

$$= -\frac{9\sqrt{3}}{2\pi^2\theta^2}\left[\frac{\sqrt{2}\pi}{8} - \frac{\sqrt{2}\pi}{8}\right] = 0 \qquad (3.40)$$

Again,

$$\tau_{xx}(x) = -\frac{9\sqrt{3}}{2\pi^2\theta}\left(\frac{1}{2}\right)^{h(x)}\left[\frac{\Gamma(\frac{1}{3})}{3\theta^{\frac{1}{3}}(x)^{\frac{1}{3}}} - \int_0^\infty \frac{e^{-\theta|x|\rho^3}\,d\rho}{\rho^8 - \sqrt{3}\rho h(x) + 1}\right] \qquad (3.41)$$

So that

$$\tau_{xx}(x) \to -\frac{9\sqrt{3}}{2\pi^2\theta}\left[\left(\frac{1}{2}\right)^{h(x)}\frac{\Gamma(\frac{1}{3})}{3^{\frac{1}{3}}(x)^{\frac{1}{3}}} - \frac{\sqrt{2}\pi\cos\frac{\pi}{8}}{4}\right] \text{ as } |x| \to 0 \qquad (3.42)$$

In summary then $\bar{\tau}(x)$ and its derivative are continuous on $(-\infty,\infty)$, but $\bar{\tau}_{xx}(x) = 0(1/|x|^{1/3})$ or $0(1/|x-x_s|^{1/3})$ as x tends to 0 or x_s, respectively.

IV. NUMERICAL TECHNIQUE

The numerical technique of Napolitano et. al. [8,9], when applied to the triple deck equations for subsonic flow past a parabolic hump, successfully accounted for the discontinuous pressure gradients at the leading and trailing edges of the hump. Therefore, it could be reasonably expected to be applicable to the present strong slot injection problem by changing the wall boundary condition for the normal velocity component. However, another modification was found necessary, i.e. the downstream boundary condition for the displacement thickness δ had to be applied as a derivative one, $\frac{d\delta}{dx} = 0$, in order to obtain correct results. This was needed because, due to the injected fluid, δ decays to zero very slowly as $x \to \infty$. When δ was set equal to zero at a finite downstream location, very inaccurate results were produced, probably due to an artifical blockage of the flow. The derivative condition was instead quite satisfactory and was used throughout this study. In the results section, the wall shear distribution obtained by this technique for $V_w = 0.1$ is shown to be in good agreement with the linear solution. However, for larger values of the injection velocity V_w, the slower convergence rate of the numerical technique, together with the necessity of imposing the upstream and downstream boundary conditions farther away from the slot, caused the computational time to become prohibitive. An effort was made therefore to remove these two major limitations. A stretching transformation of the longitudinal coordinate x was used (as in Ref. 6), to reduce the number of computational grid points without affecting the accuracy. Also, a direct (non-iterative) solution of the second sweep equation was employed to enhance the convergence rate. The numerical technique as modified for the present problem is outlined below, details being provided only for the new features.

A relaxation-like time derivative of the displacement thickness δ was added to the right hand side of the momentum equation (2.1b) so that

$$uu_x + vu_y = -\frac{dp}{dx} + u_{yy} + \frac{\partial \delta}{\partial t} \quad . \tag{4.1}$$

Then, a two-sweep Alternating Direction Implicit (ADI) technique, which is accurate to second order in time, was used; the computation proceeded from time t^n to time $t^* = t^n + \frac{\Delta t}{2}$ and from t^* to $t^{n+1} = t^* + \frac{\Delta t}{2}$ as follows:

$$(uu_x + vu_y - u_{yy})^* = -\left(\frac{dp}{dx}\right)^n + \lambda(\delta^* - \delta^n) \tag{4.2}$$

and

$$(uu_x + vu_y - u_{yy})^* = -\left(\frac{dp}{dx}\right)^{n+1} + \lambda(\delta^{n+1} - \delta^*) \quad , \tag{4.3}$$

with $\lambda = \frac{\Delta t}{2}$. (4.4)

In practice, at the * time level $\left(\frac{dp}{dx}\right)^n$ and δ^n are known at all the x_i locations and equation (4.2) is solved, coupled with the continuity equation (2.1a), by finite difference methods. These provide the u^*, v^* and δ^* arrays. This step is identical to that used by Napolitano [6] to solve the supersonic mainstream strong injection problem and those details will not be repeated here. A second sweep equation for the ADI procedure is needed to obtain the new time level values of $\left(\frac{dp}{dx}\right)^{n+1}$ and δ^{n+1}. The whole process can then be repeated until a suitable convergence criterion is met. Such an equation is obtained from equations (4.2), (4.3) and the interaction law, equation (2.6) as follows: since $\frac{dp}{dx}$ and δ do not depend on the normal coordinate y, equations (4.2) and (4.3) were combined so as to eliminate all of the velocity terms,

$$\left(\frac{dp}{dx}\right)^{n+1} = \left(\frac{dp}{dx}\right)^{n} + \lambda(\delta^{n+1} - 2\delta^{*} + \delta^{n}) \quad . \tag{4.5}$$

Then, this expression for $\left(\frac{dp}{dx}\right)^{n+1}$ is introduced into the interaction law equation (26) which is also evaluated at the n+1 time level. This gives

$$\left(\frac{d^2\delta}{dx^2}\right)^{n+1} = -\frac{1}{\pi} \oint_{-\infty}^{\infty} \frac{\left(\frac{dp}{d\xi}\right)^{n} + \lambda(\delta^{n+1} - 2\delta^{*} + \delta^{n})}{x-\xi} \, d\xi \quad . \tag{4.6}$$

Next, equation (4.6) is solved for δ^{n+1} and the pressure gradient $\left(\frac{dp}{dx}\right)^{n+1}$ is evaluated explicitely by means of equation (4.5), which completes the two sweep ADI process. Note that equation (4.6) is a second order differential equation and can satisfy both the upstream and downstream boundary conditions on δ. Together, these constitute a properly formulated two-point boundary value problem. In order to obtain the δ^{n+1} array, by numerically solving equation (4.6), the integration domain is limited to a finite range x_1, x_I where x_1 and x_I are locations sufficiently far upstream and downstream of the slot, respectively. Equation (4.6) is then modified to

$$\left(\frac{d^2\delta}{dx^2}\right)^{n+1} + \frac{\lambda}{\pi} \oint_{x_1}^{x_I} \frac{\delta^{n+1}}{x-\xi} \, d\xi = -\frac{1}{\pi} \oint_{x_1}^{x_I} \frac{(dp/d\xi)^{n} + \lambda(\delta^{n} - 2\delta^{*})}{x-\xi} \, d\xi \tag{4.7}$$

In References (8,9) it was shown that the error in the Cauchy integral due to the omitted integration $(-\infty, x_1)$ and (x_I, ∞) was negligible for a proper choice of x_1 and x_I. In the present study, it was also verified that moving x_1 and x_I farther from the slot did not produce any significant change in the results. In equation (4.7), the Cauchy integral has been split in order to place the unknown terms on the left-hand side of the equation. The Cauchy integrals here were reduced to finite difference form by the methods given in Reference 9, i.e., the δ and $(dp/d\xi)^{n}$ functions were taken as constant over each mesh of the

computational domain and removed, so that the singular terms, $\frac{1}{x-\xi}$, could be integrated analytically from each grid point to the following one. This provided the proper coefficient for the previously extracted δ_i^n and $(\frac{dp}{d\xi})_i^n$ values. Also, $(\frac{d^2\delta}{dx^2})^{n+1}$ was expressed in finite difference form using the variable grid second order accurate representation of Blottner [10] i.e.

$$\frac{2}{(x_{i+1}-x_{i-1})}\left\{\frac{\delta_{i-1}}{x_i-x_{i-1}} - \delta_i\left(\frac{1}{x_i-x_{i-1}} + \frac{1}{x_{i+1}-x_i}\right) + \frac{\delta_{i+1}}{x_{i+1}-x_i}\right\} . \qquad (4.8)$$

As described above, equation (4.7) is reduced to a system of linear algebraic equations of the form:

$$A_{ij}\ \delta_j^{n+1} = \tilde{D}_i \quad , \qquad (4.9)$$

whose solution finally provides the sought after δ_i^{n+1} array. The main difference between this technique and that of References (8,9) lies in the solution procedure for equation (4.9). This will now be discussed.

In References (8,9) an iterative procedure was used to solve the system (4.8) at every n+1 time level. Equation (4.9) was first rewritten as

$$[T_{ij} + (A_{ij} - T_{ij})]\ \delta_j^{n+1} = \tilde{D}_i \quad , \qquad (4.10)$$

where T_{ij} is the tridiagonal matrix containing all the A_{ij} elements belonging to its main, upper and lower diagonals. The $(A_{ij} - T_{ij})\ \delta_j^{n+1}$ contributions were then evaluated at a previous iteration level and combined with the known right-hand side vector $\tilde{D}_i$ to give

$$T_{ij}\ \delta_j^{n+1} = \tilde{D}_i - (A_{ij} - T_{ij})\ \delta_{pj}^{n+1} \qquad (4.11)$$

This was solved repeatedly by the very fast Thomas Algorithm until a convergence criterion for $\delta_{p_j}^{n+1}$ and δ_j^{n+1} was satisfied.

In the present technique the matrix A_{ij}, which does not depend on the solution and is therefore the same at every n+1 time level, is inverted once and for all at the beginning of the computer program. The inversion is obtained by means of the Fortran double precision version of the IMSL LIB1-0006 LINV2F subroutine designed for ill-conditioned matrices such as the present one. It uses the Gauss elimination procedure with iterative improvements until the inverse A_{ij}^{-1} is correct to a prescribed number of significant figures (chosen here to be eight). By using this inverse, the solution of the second sweep equations involved only a very fast direct matrix multiplication, i.e.

$$\delta_i^{n+1} = A_{ij}^{-1} \tilde{D}_j \tag{4.12}$$

In practice, the matrix A_{ij} was reduced to a I-2 by I-2 square matrix, I being the total number of grid points in order to properly satisfy the boundary conditions on δ^{n+1}. These conditions were taken to be $\delta(x_1) = 0$ and $\frac{d\delta}{dx}(x_I) = 0$, respectively, which in finite difference form became

$$\delta_1 = 0 \quad ; \quad \delta_I = \delta_{I-1} \tag{4.13a,b}$$

The I by I to I-2 by I-2 matrix reduction, needed to enforce equations (4.13a,b) is very straightforward and is omitted here. Note that in equation (4.12) the indexes i and j vary between 2 and I-1. In the computer program they were all reduced by one to accommodate the Fortran language implementation.

In Reference (9) it was shown that for a constant step size all the logarithms needed for evaluating the Cauchy Integrals in equation (4.6) need be evaluated only once and stored in a vector of dimension 2I. In this way the computational effort was reduced drastically with respect to evaluating all the logarithms at every second sweep of the solution process. In the present study

due to the variable grid distribution, a I by I matrix was necessary to store all the above mentioned logarithms.

In the results section it can be seen that the improved algorithm was able to compute the solution for $V_w = 1.5$ in a reasonable CPU time. The technique of References (8,9) in this case, would have required a significantly higher computer storage space and a CPU time one order of magnitude higher.

V. RESULTS

a) Linear Equations Results

A small computer program was used to evaluate the linear theory pressure and wall shear given by equations (3.31, 3.32) and (3.36, 3.37). All the integrals were evaluated by the simple trapezoidal rule with the range of integration for ρ limited to $0 \leq \rho \leq \rho_{max} = 100$. It can be seen that this approximation leads to an error of order ρ_{max}^{-4} or less, which is obviously negligible. However, the integrand of the integral,

$$I = \int_0^\infty \frac{\sqrt{3}/2\ \rho^6 - \rho^2}{\rho^8 - \sqrt{3}\ \rho^4 + 1}\, d\rho \tag{5.1}$$

is of order $\frac{1}{\rho^2}$ as $\rho \to \infty$. This appears in the expression for the wall shear $\bar{\tau}_w$, equation (3.36), when either x or $x-x_s$ are equal to zero. It is easily seen that,

$$I = \int_0^{\rho_{max}} \frac{\sqrt{3}/2\ \rho^6 - \rho^2}{\rho^8 - \sqrt{3}\rho^4 + 1}\, d\rho + \int_{\rho_{max}}^\infty \sqrt{3}/2\ \rho^{-2}\, d\rho + O(\rho_{max}^{-5}) \tag{5.2}$$

Therefore a very accurate evaluation of I can be obtained by using the trapezoidal rule numerical integration for the first term in the right-hand side and adding to it the second term contribution of $\sqrt{3}/(2\rho_{max})$. A step size $\Delta\rho = 0.02$ was used for the numerical integration throughout. Smaller values for $\Delta\rho$ were found to change the numerical results only in the seventh or eight significant figure. The numerical evaluation of $\bar{p}(0)$ provided agreement to eight digit accuracy with the analytical value given in section III. Furthermore, $\bar{p}(0)$ and $\bar{\tau}(0)$ were evaluated using both of the expressions valid for $x = 0-$ and $x = 0+$. The two results coincided up to the seventh digit, again showing very good accuracy.

The results for $\bar{\tau}_w$ and $p(x)$ corresponding to a wide range of slot lengths x_s are presented in figures 2 and 3, where all the features anticipated in Section III can be easily observed. In particular, it is interesting to notice the asymptotic tendency of the results for finite x_s toward that of the limiting case for $x_s \to \infty$. Also of interest is the fact that the present results are qualitatively very similar to those obtained by Smith and Stewartson [4] for the supersonic mainstream case. A noticeable difference is that the supersonic mainstream pressure ahead of the slot $[\bar{p} = \frac{3}{4\theta}(e^{x} - e^{(x-x_s)})]$ is essentially independent of the slot length x_s for $x_s > 5$. In the subsonic mainstream case the pressure rise ahead of the slot is spread out over a much longer region and it changes much more significantly as x_s grows larger. This is consistent with the fact that in subsonic maintream flow disturbances usually can extend upstream over a longer region. Incidentally, note that the graphical results in Reference 4 are scaled with respect to the $\bar{p}(0)$ and $\bar{\tau}(0)$ values, respectively, so that $\bar{p}(x)$ and $\bar{\tau}(x)$ appear to be independent of x_s, which is untrue. It should also be pointed out that very similar results for the supersonic and subsonic mainstream cases were found by Smith [11] for the problem of flow past a small hump on a flate plate. For that case Napolitano et. al. [8] also found that such a similarity was maintained by the nonlinear results, and actually for both cases separation first occurred at the downstream side of the hump as anticipated by linear theory. For the supersonic slot injection problem Napolitano [6] has found that, due to nonlinear effects, separation first occurs ahead of the slot for a length of the same, $x_s = 5$. An even more remarkable result, for the present subsonic mainstream case, is discussed next.

b) Nonlinear Equations Results

Solutions to the nonlinear equations are presented for one slot length only $x_s = 5$. A comparison can then be made with the supersonic mainstream results of Napolitano [6], particularly with respect to the occurrence and location of separation. A small value of the wall injection velocity ($V_w = 0.1$) was chosen first, in order to check accuracy and reliability of the numerical technique by comparison with the linear theory results. Both the numerical technique of References [8, 9] with the appropriate boundary conditions, as described in section IV, and the new one using a variable grid and a direct inversion of the second sweep equation were used for this check. The wall shear results obtained by the two different programs are shown in figure 4 together with the linear results. The agreement between linear and nonlinear solutions is quite satisfactory, considering that the nonlinear solutions are only first order accurate in the longitudinal direction x and use a fairly large step size $\Delta x = 0.25$; also, for $V_w = 0.1$ linear theory could have some error. Moreover, the agreement between the two nonlinear solutions is almost perfect, considering the several differences between the two schemes. For the first one, for example, the step size Δx was constant everywhere ($\Delta x = 0.25$), x_1 and x_I were equal to -10 and 15 respectively, and the second sweep equation was modified according to the way described in Reference 8, section IVc. The new scheme, instead, used step size Δx variable outside the slot, according to the stretching provided in Reference 6. x_1 and x_I were equal to -20.8 and 25.8 respectively and the Cauchy integral of a discontinuous pressure gradient is evaluated according to the method described in Reference 9, section IV 3. The pressure profiles were also found to be in close

agreement. A step size study was performed for the new numerical scheme. The results for the shear and pressure at the leading edge of the slot are shown in Figure 5; the second order accuracy in the normal direction y and the first order accuracy in the longitudinal direction x are clearly verified. The new technique was then employed to obtain numerical solutions for larger values of the injection velocity. The wall shear distributions obtained for three values of V_w, namely 0.5, 1 and 1.5, are presented in figure 6. These results are very interesting and quite surprising. As in the supersonic mainstream case [6] the wall shear decreases monotonically upstream of the slot and has a dip immediately after the front of the slot. It then decreases again along most of the slot length. In the supersonic free stream problem, as V_w increased to a value of about 1.1 the minimum shear became negative just ahead of the slot indicating the occurrence of separation and a small region of negative shear was found ahead and through the slot frong for $V_w = 1.5$. In the present problem the shear dip ahead of the slot also increases with V_w and separation would appear likely there for a large enough V_w value. However, in this case, a new feature appears, i.e., there is a more rapid shear decrease downstream of the slot as V_w increases. This is small and very localized for $V_w = 0.5$ but it becomes more and more significant as V_w increases. For $V_w \cong 1.3$, the shear actually goes to zero downstream of the slot and for $V_w = 1.5$ a reverse flow bubble is present over a fairly large distance on the plate.

All the results have been obtained using a constant step size in the normal direction y, $\Delta y = 0.3$ and a variable one in the longitudinal direction x, $\Delta x \geq 0.25$. The values for x_1 and x_I where taken to be $-20.8, -30, -35.2$ and $25.8, 35, 45.8$ corresponding to $V_w \leq 0.5$, $V_w = 1$ and $V_w = 1.5$, respectively.

The outer edge boundary conditions were imposed at y = 12, 15, 18 and 21 corresponding to V_w = 0.1, 0.5, 1 and 1.5. In all cases the solution did not change appreciably when the domain of integration was increased. Two points are of special interest. First, due to the direct inversion of the second sweep equation the optimal time step for convergence was found to be equal to two. This is the same as in the supersonic mainstream case [6]. (For the technique of References (8,9) it was equal to one). Second, the convergence rate here was comparable to that for the supersonic mainstream. For $V_w \leq 1$ the average variation for δ over one complete time step became of the order of 10^{-7} in less than one hundred iterations. For V_w = 1.5 the convergence rate was much slower so that it had to be reduced to one. In all, 500 iterations were required for a total computational time of about 8 CPU, on the AMDAHL/470 computer. The solution was initialized with the uniform shear flow configuration (u = y, v = δ = dp/dx = 0 every where). The injection velocity V_w was started at the value of 0.1 and increased by 0.1 after each time step until the final, desired value, was reached.

VI. REFERENCES

1. Rosenhead, L, (Ed.), Laminar Boundary Layers, Oxford University Press, Oxford, 1966.

2. Stewartson, K. and Williams, P.G., "Self Induced Separation," Proc. Roy. Soc. London, Ser. A, Vol. 312, 1969, pp. 181-206.

3. Stewartson, K., "Multistructured Boundary Layers on Flat Plates and Related Bodies," Advances in Applied Mechanics, Vol. 14, Academic Press, 1974, pp. 145-239.

4. Smith, F.T. and Stewartson, K., "On Slot Injection Into a Supersonic Laminar Boundary Layer," Proc. Roy. Soc. London, Series A, Vol. 332, 1973, pp. 1-22.

5. Smith, F.T. and Stewartson, K., "Plate Injection Into a Separated Supersonic Boundary Layer," Journal of Fluid Mechanics, Vol. 58, Part 1, 1973, pp. 143-159.

6. Napolitano, M., "A Numerical Study of Strong Slot Injection Into a Laminar Boundary Layer," AIAA Paper 79-0142, presented at the AIAA 17th Aerospace Sciences Meeting, New Orleans, Louisiana, January 15-17, 1979.

7. Sychev, V. Ya., "Concerning Laminar Separation," Izv. Akad. Naut. SSSR, Mekh, Zhidk Gaza, No. 3, 1972, pp. 47-59.

8. Napolitano, M., Werle, M.J. and Davis, R.T., "A Numerical Technique for the Triple Deck Problem," AIAA Paper 78-1133, presented at the AIAA 11th Fluid and Plasmadynamics Conference, Seattle, Washington, July 1978.

9. Napolitano, M., Werle, M.J. and Davis, R.T., "Numerical Solutions of the Triple-Deck Equations for Supersonic and Subsonic Flow Past a Hump," University of Cincinnati, Dept. of Aerospace Engineering AFL Report No. 78-6-42, June 1978.

10. Blottner, F.G., "Computational Techniques for Boundary Layers," AGARD Lecture Series No. 73, February 1975.

11. Smith, F.T., "Laminar Flow Over a Small Hump on a Flat Plate," J. Fluid Mech., 57, 1973, pp. 803-829.

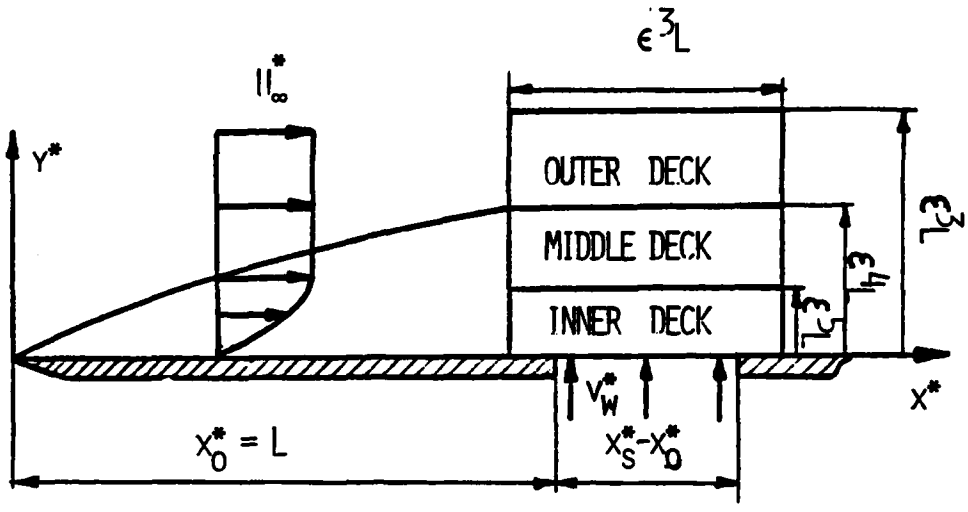

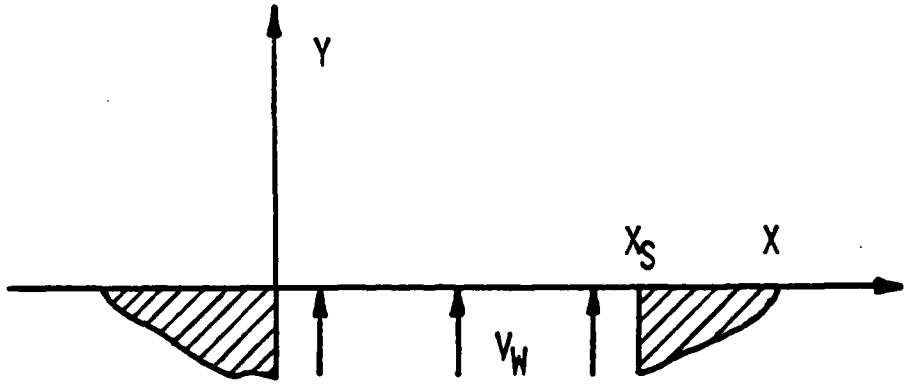

Figure 1. THE STRONG SLOT INJECTION PROBLEM

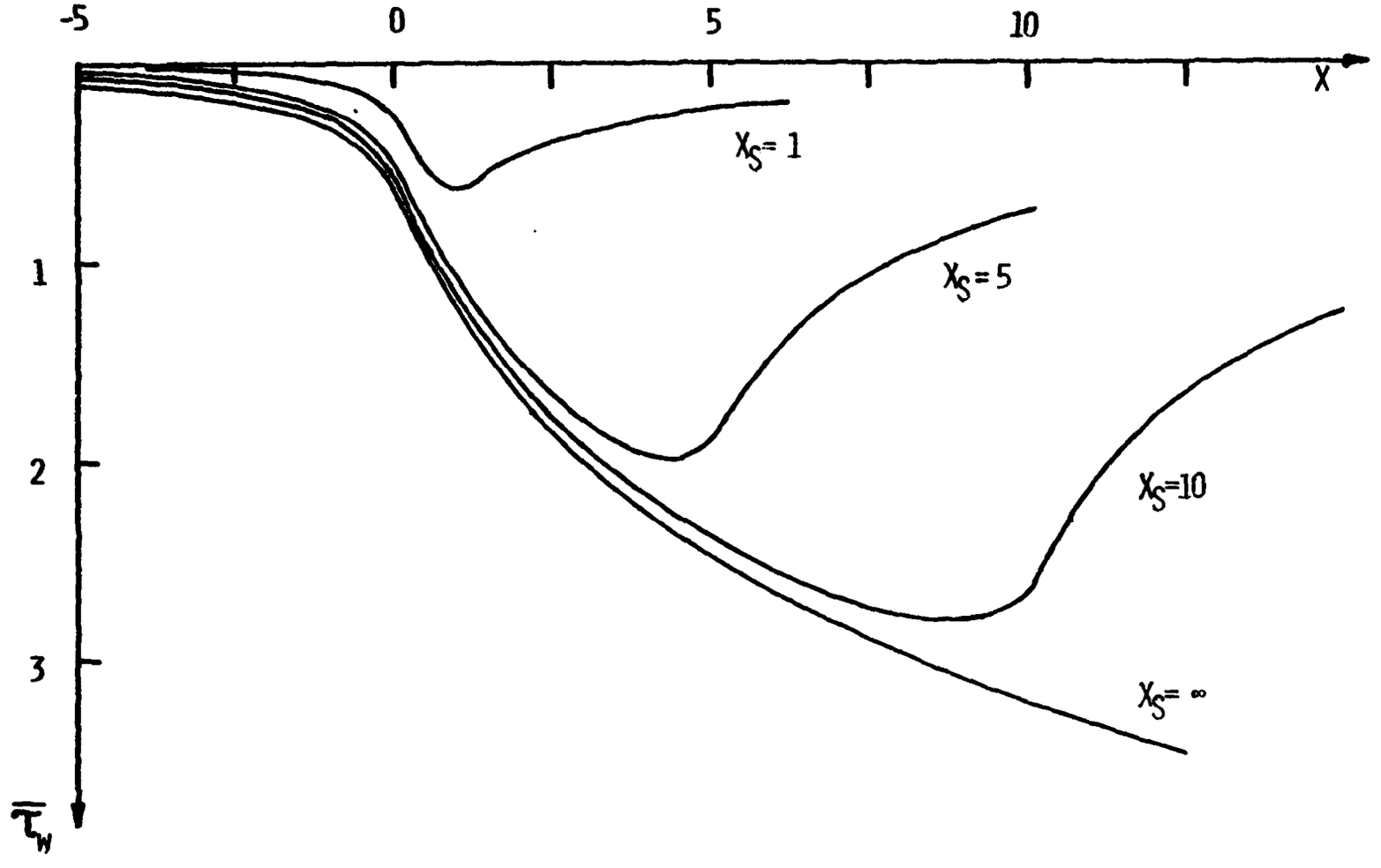

Figure 2. LINEAR PROBLEM WALL SHEAR PROFILES

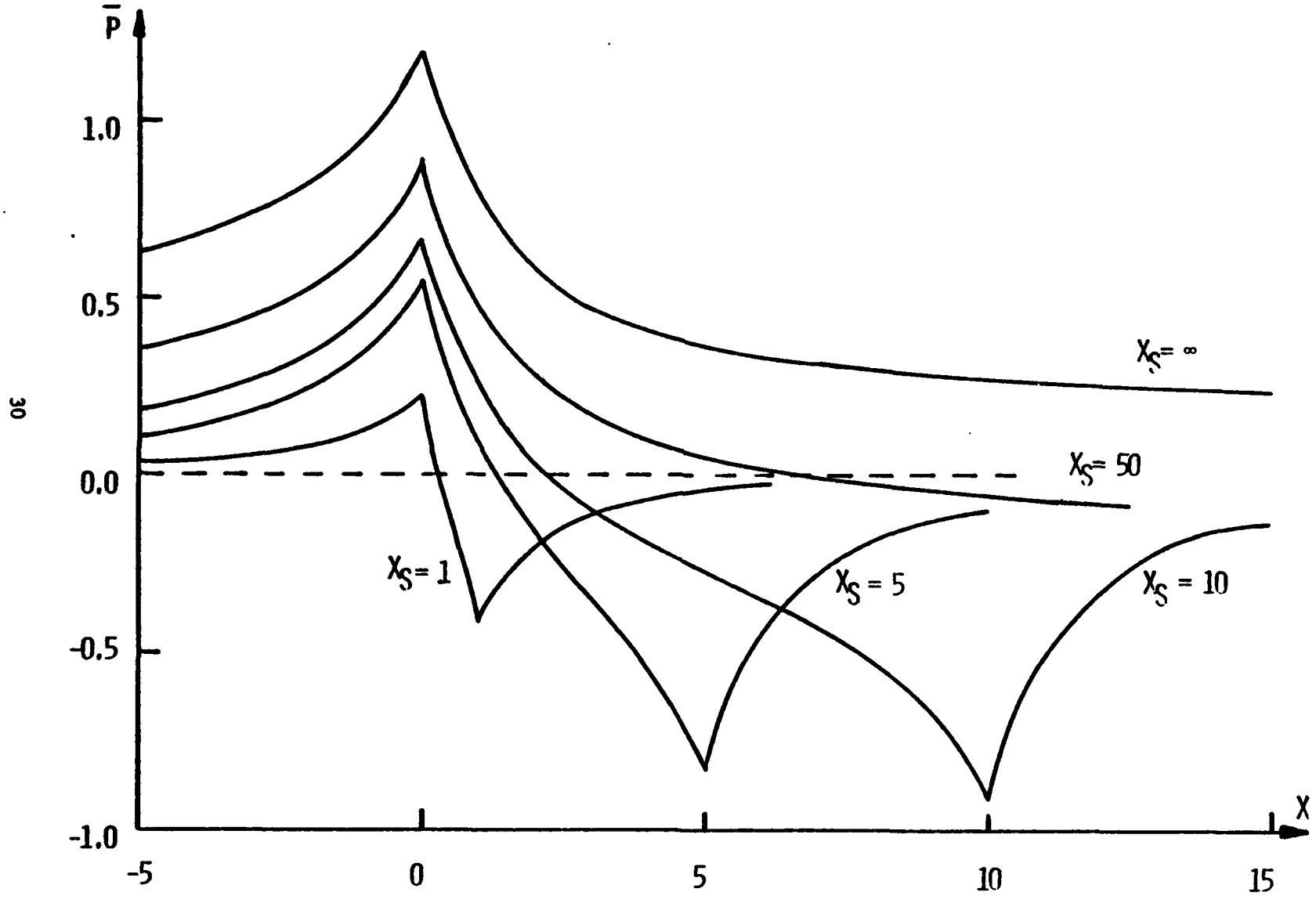

Figure 3. LINEAR PROBLEM PRESSURE PROFILES

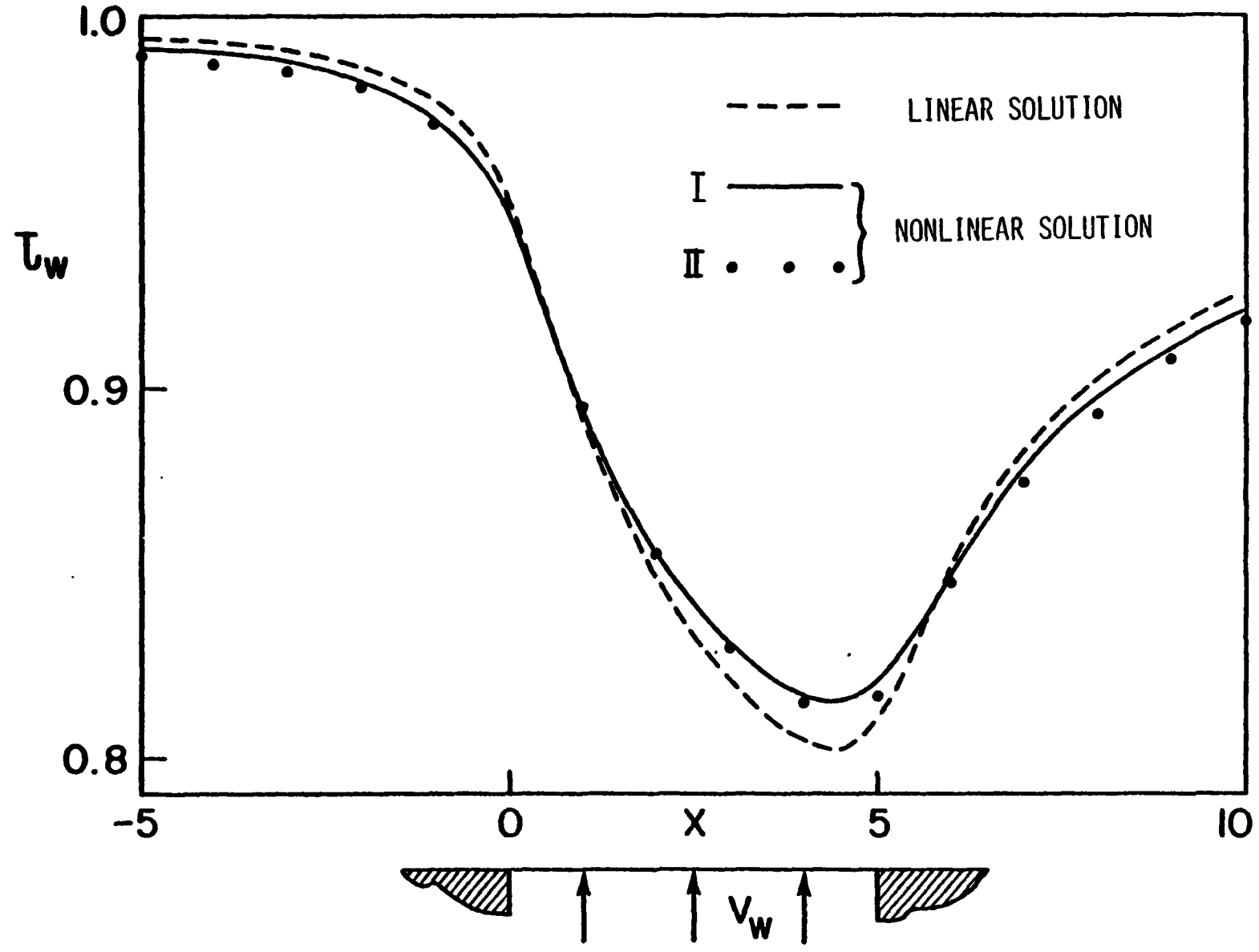

Figure 4. x_s=5, V_w=0.1, NONLINEAR AND LINEAR WALL SHEAR RESULTS

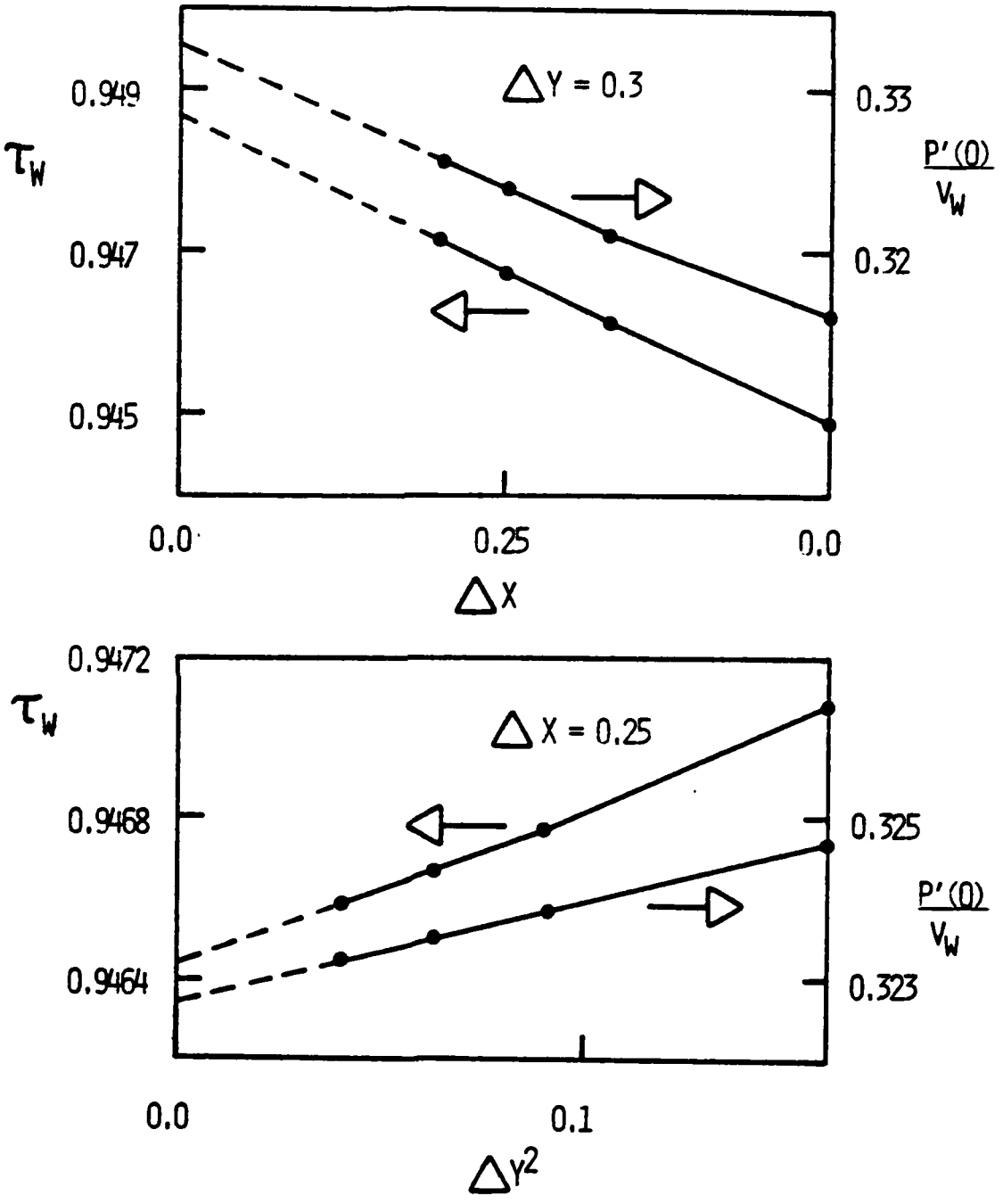

Figure 5. x_s=5, V_w=0.1, STEP SIZE STUDIES

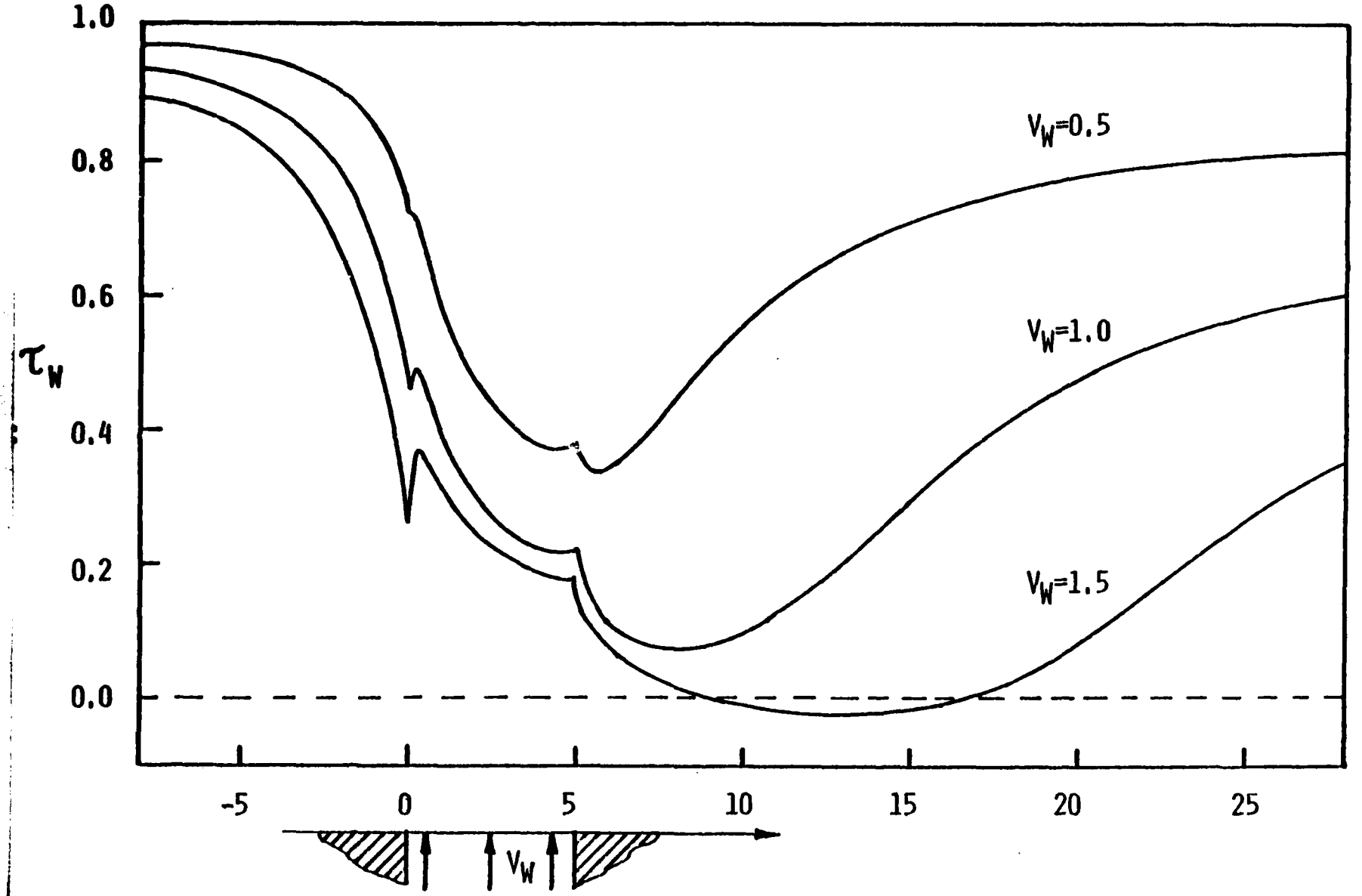

Figure 6. x_s=5. WALL SHEAR DEPENDENCE ON V_w